MODELLING OF CUTTING PROCESS WITH COOLING

Wojciech Zębala

Summary

This investigation concerns an analysis of nickel alloy Inconel 718 machining in different cooling cases: immerse cooling, cooling of a specific area of the cutting zone and dry cutting. Simulation of turning process with a sintered carbide tool coated by TiAlN layer at cutting speed v_c = 80 m/min, feed f = 0,12 mm/rev and depth of cut a_p = 2 mm was perform. In calculations a finite element method was used. The results of calculations are presented in the form of temperature and von Mises stress distributions.

Keywords: modeling, cutting, cooling

Modelowanie procesu skrawania z chłodzeniem

Streszczenie

Praca dotyczy analizy obróbki skrawaniem stopu niklu Inconel 718 dla takich sposobów chłodzenia, jak: chłodzenie zalewowe, chłodzenie określonego obszaru strefy skrawania oraz skrawanie na sucho. Przeprowadzono symulację procesu toczenia narzędziem z węglików spiekanych z powłoką TiAlN dla prędkości skrawania v_c = 80 m/min, posuwu f = 0,12 mm/obr i głębokości skrawania a_p = 2 mm. W obliczeniach stosowano metodę elementów skończonych. Przedstawiono rozkład wartości temperatury i naprężeń wg hipotezy Hubera.

Słowa kluczowe: modelowanie, skrawanie, chłodzenie

1. Introduction

Many machining researches are focused on cutting process, especially on cutting tools mainly due to the wear developed as a result of high temperatures generated that accelerate thermally related wear mechanisms, consequently reducing tool life. Cutting fluids are used in machining operations to minimize cutting temperature, through the profitable arrangement of thermal streams flowing between chip, edge and workpiece [1-4].

Generally, the cooling – lubricating liquids are responsible for: tool life increase, workpiece protection from thermal damage, lubricating of the edge, work and chip contact, decrease of the cutting resistance, chip shaping, chip

Address: Wojciech ZĘBALA, Ph.D. DSc., Cracow University of Technology, Production Engineering Institute, Al. Jana Pawa II 37, 31-864 Kraków, fax: (+48 12) 374 3202

evacuation, protection from corrosion and working space cleaning. The simplest way of coolant delivery to the cutting zone is pouring the coolant over the tool and worpkiece. It restrains only to the free flowing down of steered stream of liquid. This case of cooling gives way to other solutions [1, 2, 4]. It should be mainly involved with a fact of insufficient effectiveness and large amount of coolant 20 ÷ 50 l / min.

Today, machining is characterized by the more rational economy with liquids, getting the demanded quality of cooling joint with limited waste of factor. This depends on the coolant delivery through the jet of pipe directly to the chosen place of the cutting zone, reducing the tool temperature and chip wash away. In cases of machining in heavier conditions, where the higher thermal stresses occur, several streams are used, responsible for cooling of a specific area [4].

In this study, an analysis of Inconel 718 cutting modeling in different cooling cases is presented. Determination of cooling ability to improve the machining is the main purpose of the researches. Inconel 718 belongs to super alloys, characterizes by a big hardness and a high mechanical strength in a high temperature. This material is applied in the aerospace and automotive industries, mainly to the engine elements producing.

Alloys basing on a nickel are difficult to cut materials, because of low thermal conductivity and high chemical reactivity with many cutting tool materials. The low thermal conductivity increases temperature at the cutting edge of tool. The key limitation preventing cost-effective machining of nickel alloy is the efficient cooling of the cutting tool. Effective cooling becomes more important as processing speeds are increased to reduce costs, improve part strength, and enhance reliability.

2. Modeling of cutting process

A simulation of turning process of the Inconel 718 alloy with sintered carbide tool (insert *VCMT* with *SM* chipbreaker geometry and $\kappa_r = 90^o$ – Iscar tool) coated by TiAlN layer (5 μm thickness) at cutting speed v_c = 80 m/min, feed f = 0,12 mm/rev and depth of cut a_p = 2 mm was perform with the help of the finite element method calculations [5]. A mechanical and thermal load analysis of the rake and clearance faces for different cooling cases was taken into consideration in the model:

- immersed option,
- coolant is coming from a jet and is targed on the specific area (focused option),
- dry cutting.

Fig. 1 presents schematic heat streams flowing from the cutting zone to the surroundings for two cooling options applied in the simulation. Fig. 1a illustrates

an immersed option, however Fig. 1b presents a case of energy captured from the defined area.

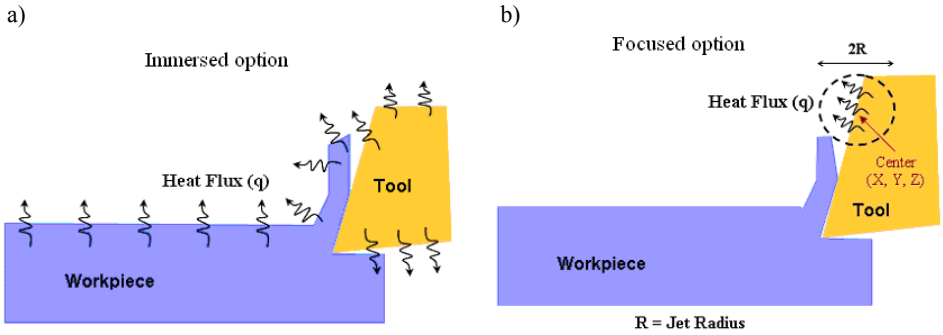

Fig. 1. Model of cutting zone for two cooling options: a) immersed option, b) focused option

The selective cooling of a defined area is realized through a suitable jet steering by which the stream of liquid sails out. Two ways of a jet situation are presented in the paper. In the first case, the cooled area has a diameter D_1 = 1 mm and its centre has coordinates X = 4,5 mm and Y = 2,3 mm, jet 1 in Fig. 2. In the second case (working of jet 2) the centre of cooled area is in the point of coordinates: X = 5 mm, Y = 2,8 mm. The diameter D_2 = 0,4 mm.

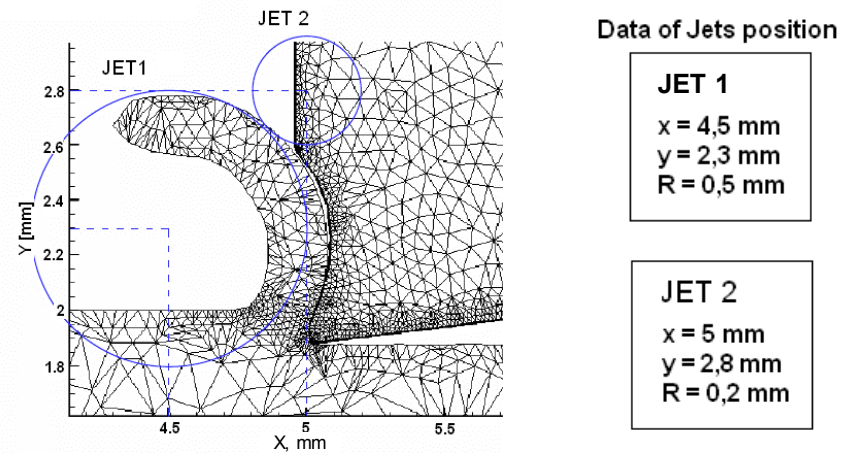

Fig. 2. Cutting zone areas cooled by jet 1 and jet 2. Position of jets: coordinates (x, y) and radius R are presented on the right side

A Lagrangian finite element method was used to the simulation of the cutting process. Equation 1 presents the constitutive model by which the material is governed.

$$\sigma(\varepsilon^p, \dot{\varepsilon}, T) = g(\varepsilon^p) * \Gamma(\dot{\varepsilon}) * \Theta(T) \tag{1}$$

where $g(\varepsilon^p)$ is strain hardening, $\Gamma(\dot{\varepsilon})$ is strain rate sensitivity and $\Theta(T)$ is thermal softening.

The strain hardening function $g(\varepsilon^p)$ is defined as (2):

$$g(\varepsilon^p) = \sigma_0 \left(1 + \frac{\varepsilon^p}{\varepsilon_0{}^p}\right)^{1/n}, \quad \text{if } \varepsilon^p < \varepsilon^p_{cut},$$
$$g(\varepsilon^p) = \sigma_0 \left(1 + \frac{\varepsilon^p_{cut}}{\varepsilon_0{}^p}\right)^{1/n}, \quad \text{if } \varepsilon^p \geq \varepsilon^p_{cut} \tag{2}$$

where σ_0 is the initial yield stress, ε^p is the plastic strain, ε^p_0 is the reference plastic strain, ε^p_{cut} is the cutoff strain and n is the strain hardening exponent.

The reference plastic strain is the strain corresponding to the initial yield stress. The strain hardening exponent decreases with increasing strain hardening dependence. The cutoff strain is used to limit the strain hardening function. After the cutoff strain has been exceeded, the model becomes perfectly plastic and has constant flow stress. This prevents large extrapolation errors at strains that are higher than tested. The rate sensitivity function $\Gamma(\dot{\varepsilon})$ is defined as (3):

$$\Gamma(\dot{\varepsilon}) = \left(1 + \frac{\dot{\varepsilon}}{\dot{\varepsilon}_0}\right)^{\frac{1}{m_1}}, \quad \text{if} \quad \dot{\varepsilon} \leq \dot{\varepsilon}_t \tag{3}$$
$$\Gamma(\dot{\varepsilon}) = \left(1 + \frac{\dot{\varepsilon}}{\dot{\varepsilon}_0}\right)^{\frac{1}{m_2}} \left(1 + \frac{\dot{\varepsilon}_t}{\dot{\varepsilon}_0}\right)^{\left(\frac{1}{m_1} - \frac{1}{m_2}\right)}, \quad \text{if} \quad \dot{\varepsilon} > \dot{\varepsilon}_t$$

where $\dot{\varepsilon}$ is strain rate, $\dot{\varepsilon}_0$ is reference plastic strain rate, $\dot{\varepsilon}_t$ is strain rate where the transition between low and high strain rate sensitivity occurs, m_1 is the low strain rate sensitivity coefficient, m_2 is the high strain rate sensitivity coefficient.

The thermal softening function $\Theta(T)$ is defined as (4):

$$\Theta(T) = c_0 + c_1 T + c_2 T^2 + c_3 T^3 + c_4 T^4 + c_5 T^5, \quad \text{if} \quad T < T_{cut} \tag{4}$$

$$\Theta(T) = \Theta(T_{cut}) - \frac{T - T_{cut}}{T_{melt} - T_{cut}}, \quad \text{if} \quad T \geq T_{cut}$$

where c_0 through c_5 are coefficients for the polynomial fit, T is the temperature, T_{cut} is the linear cutoff temperature and T_{melt} is the melting temperature.

The melting temperature means the temperature either the material melts at or where the yield stress is zero. At the cutoff temperature the yield stress is linearly softened until the yield strength is zero.

Young's Modulus and Poisson's Ratio are the variables used to compute stress in the elastic strain region until the yield stress is reached and plastic deformation begins.

The thermal conductivity function $K(T)$ is described by the following polynomial function (5):

$$K(T) = k_0 + k_1 T + k_2 T^2 + k_3 T^3 + k_4 T^4 + k_5 T^5, \quad \text{if} \quad T < T_{\max} \tag{5}$$

$$K(T) = K(T_{\max}), \quad \text{if} \quad T \geq T_{\max}$$

where k_0 through k_5 are coefficients for the polynomial fit, T is the temperature and $T_{\max}$ is the linear cutoff temperature (at this temperature and above the thermal conductivity is held constant).

The heat capacity function $C(T)$ is described by the following polynomial function (6):

$$C(T) = cp_0 + cp_1 T + cp_2 T^2 + cp_3 T^3 + cp_4 T^4 + cp_5 T^5, \quad \text{if} \quad T < T_{\max} \tag{6}$$

$$C(T) = C(T_{\max}), \quad \text{if} \quad T \geq T_{\max}$$

where cp_0 through cp_5 are coefficients for the polynomial fit, T is the temperature and $T_{\max}$ is the linear cutoff temperature (at this temperature and above the heat capacity is held constant).

The thermal expansion function $A(T)$ is described by the following polynomial function (7):

$$A(T) = a_0 + a_1 T + a_2 T^2 + a_3 T^3 + a_4 T^4 + a_5 T^5, \quad \text{if} \quad T < T_{\max} \tag{7}$$

$$A(T) = A(T_{\max}), \quad \text{if} \quad T \geq T_{\max}$$

where a_0 through a_5 are coefficients for the polynomial fit, T is the temperature and $T_{\max}$ is the linear cutoff temperature (at this temperature and above the Thermal Expansion is held constant).

3. Analysis of simulation results

Temperature and von Mises stress distributions on the clearance and rake faces of tool were drawn after numerical calculations, Fig. 4-7. Characteristic points (A, B, C) allowing identification of diagrams location (Fig. 4-7) are shown in Fig. 3. The point B lies just on the cutting edge.

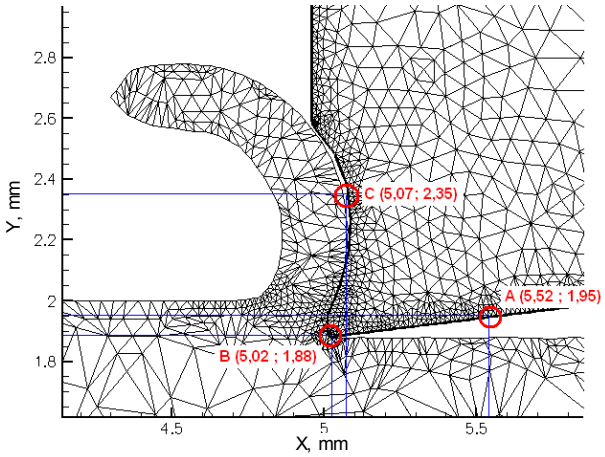

Fig. 3. Location of points A, B i C

The following Fig. 6 presents the temperature distribution in the cutting zone. Maximum temperature of value about 800°C exists on the rake face, just on the cutting edge (for dry cutting and cooling case – jet 1) or on the rake face at a distance about 0,12 mm from the cutting edge.

The ranges of graphs illustrating the changes of temperature on the clearance face do not show the clearly predominant influence of any studied ways of cooling.

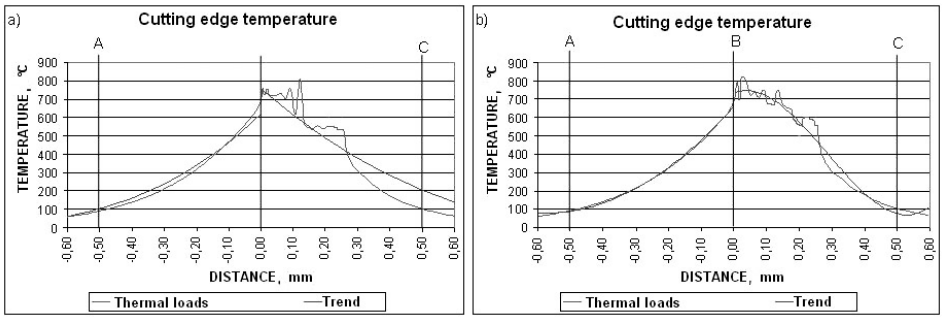

Fig. 4. Temperature distributions on the clearance and rake faces in cases:
a) immersed cooling, b) jet 1

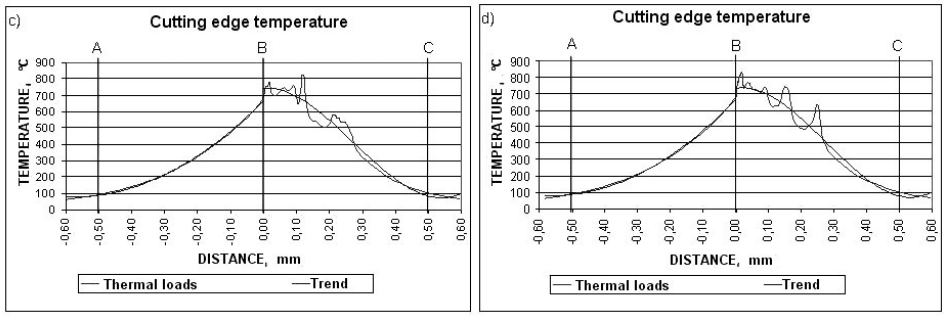

Fig. 5. Temperature distributions on the clearance and rake faces in cases:
c) jet 2, d) dry cutting

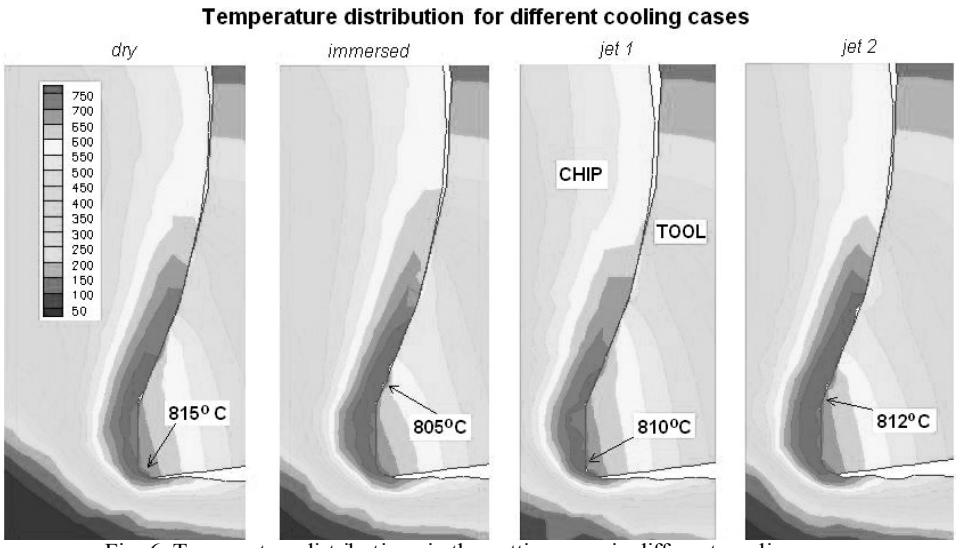

Fig. 6. Temperature distributions in the cutting zone in different cooling cases

The clear differences of cutting edge thermal load courses for individual cooling cases are visible on the rake face in the range from the point B to the distance 0,3 mm from the main cutting edge. The case of immersed cooling characterizes by the restricting of the range of temperature occurrence above 600°C to the 0,13 mm width (measured from the point B). The similarly regularity accompanies the case of cooling by the jet 2.

The trend line shown in Fig. 5a, especially ascribed for the rake face, indicates a relatively effective influence of immersed cooling on the edge thermal load decrease.

The presented profiles, describing the case of dry cutting do not show the strongly negative influence of a lack of cooling on the thermal load distribution on the cutting edge surfaces. The discussed dependence has an approximate schedule to the profiles ascribed to the jet1. It has a less dynamic course, devoid of frequent local extremes.

The profiles of von Mises stress on the rake face, visible in Fig. 7-8, indicate the similar character of value distributions for the individual cooling cases of cutting zone. The maximum value of the stress exists very close to the main cutting edge (point B) or in the close neighborhood on the rake face. The sudden value growth to the maximum level and then the violent fall to the level about 3000 MPa marks all the presented graphs.

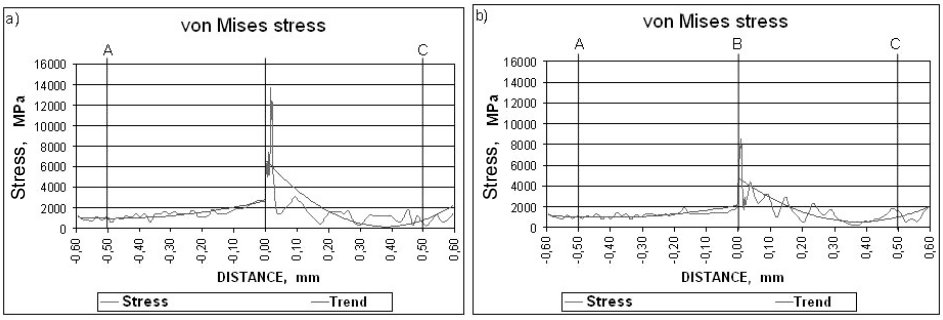

Fig. 7. Von Mises stress distributions on the clearance and rake faces in cases: a) immersed cooling , b) jet 1

The stress reaches a maximum value about 14000 MPa during dry cutting, immersed cooling as well as during cooling by jet 2. In case of cooling by the jet 1 a considerable lower stress value – 8000 MPa is reached. The visible trend lines on the rake face answer the value decrease in the range of 0,4 mm from the point B (cutting edge).

Numerical calculations of cutting forces (F_c and F_f) are shown in Tab. 1. The lowest values of forces occurred in case of cooling – jet 1. The same tendency was observed for von Mises stress (Fig. 7b).

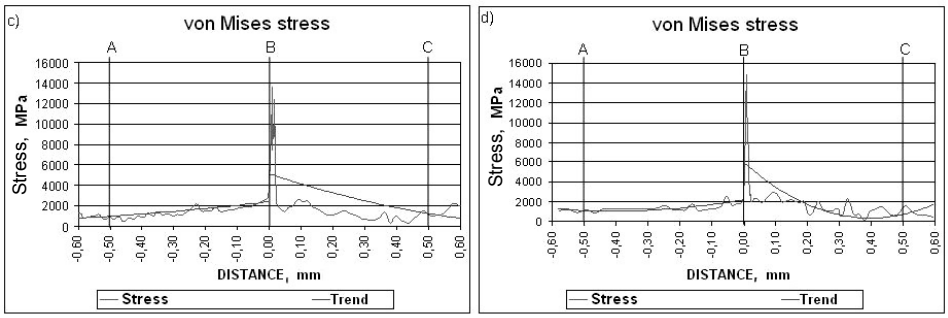

Rys. 8. Von Mises stress distributions on the clearance and rake faces in cases: c) jet 2, d) dry cutting

Tab. 1. Main F_c and feed F_f cutting forces for different cooling cases

Case of cooling	F_c **[N]**	F_f **[N]**
Immersed	1050	540
Jet 1	1030	520
Jet 2	1060	550
Dry	1070	560

Basing on the analysis of temperature and stress distributions it can be affirmed the case of cooling – jet 1 gives the most profitable cutting conditions: the lowest stress and forces (the lowest weaken of the cutting edge) as well as comparable values of cutting edge temperature. Additionally in this case the highest temperature is not generated directly on the cutting edge but in the certain distance from it.

References

[1] L. DOBRZYŃSKI, J. MIKUŁA, M. SOKOVIĆ: Struktura i własności tlenkowej ceramiki narzędziowej Al_2O_3 + TiC z powłokami PVD i CVD do skrawania na sucho z dużymi prędkościami. *Mechanik*, (2005)4, 309-315.
[2] K. JEMIELNIAK: Obróbka na sucho i z minimalnym smarowaniem. Mat. Konf. „Innowacyjne technologie w budowie maszyn", Poznań 2005.
[3] K.E. OCZOŚ: Postęp w obróbce skrawaniem – obróbka na sucho i ze zminimalizowanym smarowaniem. *Mechanik*, (1998)5-6, 307-318.
[4] K.E. OCZOŚ: Doskonalenia strategii chłodzenia i smarowania w procesach obróbkowych. *Mechanik*, (2004)10, 597-607.
[5] User's Manual of AdvantEdge v5.2 machining simulation software, Minneapolis 2008.

Received in December 2008